Fitting Wake-Up Radio Communication in ISM Bands by Employing Signal Shaping

Robert Fromm
Faculty of Engineering
Leipzig University of Applied Sciences
Leipzig, Germany
0000-0002-2905-0648

Olfa Kanoun
Department of Electrical Engineering and Information Technology
Chemnitz University of Technology
Chemnitz, Germany
0000-0002-7166-1266

Faouzi Derbel
Faculty of Engineering
Leipzig University of Applied Sciences
Leipzig, Germany
0000-0002-7038-8157

Note: This is the manuscript version of this publication. See https://doi.org/10.1109/I2MTC62753.2025.11079058 for the published version. Current version: July 24, 2025.

***Abstract*—Wake-up receivers (WuRxs) enable wireless, low-latency communication with greatly improved power efficiency, operating up to a thousand times more efficiently than conventional RF receivers. WuRxs are typically designed to operate in license-free RF bands (ISM bands). Many studies report improvements in WuRx designs regarding sensitivity, latency, and power consumption. However, detailed characterizations of the wake-up packets (WuPts) used are often missing. We proposed a measurement setup to accurately and repeatably measure the bandwidth of the WuPt. We found high bandwidth requirements of many WuPts used in current research. The bandwidth of these WuPts is wider than the frequency span of the utilized RF band. We also conducted a theoretical analysis to explain why WuPts tend to have high bandwidth. We performed bandwidth measurements on WuPts generated by different RF transmitters, including a lab-grade vector signal generator and two commercially available RF transceiver ICs. Finally, we implemented pulse shaping in all three devices. With pulse shaping, we were able to reduce the bandwidth requirements to 25% or even to 50%.**

***Index Terms*—Wake-up receiver, wireless sensor network, ultra-low power, low-frequency receiver, AS3933, on-demand communication, bandwidth**

I. Introduction

Long-lasting battery life in wireless sensor nodes is essential for modern wireless sensor networks. The reception mode of the sensor node is known to consume the most power. While continuous data reception is desirable, it is incompatible with achieving multi-year battery life [1]. Even modern RF transceivers consume more than 10 mW during continuous reception, making a duty-cycling approach necessary to reduce power consumption significantly. However, this approach increases latency in event-driven communication, making battery-powered systems unsuitable for many real-time applications [2].

This research is financed by the Saxon State government out of the State budget approved by the Saxon State Parliament.

Several recent publications suggest using wake-up receivers (WuRxs), which are specialized RF receivers with a power consumption below 10 µW. This low power consumption enables continuous and energy-efficient reception. WuRxs are typically designed to receive only dedicated RF packets, known as wake-up packets (WuPts), and are integrated alongside the main radio in the sensor node. [3]–[5]

Recent publications introduce various WuRx prototypes, often based on application-specific integrated circuits (ASICs) [6]. However, we focus on WuRx devices built from commercial off-the-shelf (COTS) components. These devices are notable for their simplicity, requiring minimal components while ensuring interference-free communication [7]–[9].

The main performance parameters of WuRxs are sensitivity, power consumption, and latency [10]. Most articles focus on optimizing these parameters. In this article, however, we focus on the generation of WuPts. Our analysis of existing research found that only a minority of articles provide details on WuPt generation. We assert that this is the first article on COTS WuRxs to provide WuPt bandwidth measurements.

Measuring RF bandwidth is essential to ensure that WuPts fit into license-free RF bands or industrial, scientific, and medical (ISM) bands. We will show that a large portion of the WuPts in current research have a higher bandwidth than the frequency span of the utilized RF band. This compliance test ensures that WuRxs can be used legally across a wide range of applications and supports their broader adoption in practical applications in the future.

This article is structured as follows. In Section II, we presented the state of research. In Section III, we analyze the bandwidth requirements of the WuPts theoretically. In Section IV, we present the methodology of our bandwidth measurements and the RF transmitters used to generate the test packets. In Section V, we present the results of our bandwidth measurements. We employ shaping filters to reduce the bandwidth of the WuPts. The article is summarized in Section VI. Additionally, we discuss the importance of the bandwidth reduction for the different typically used frequency bands.

II. State of Research

The majority of COTS WuRxs rely on a passive radio-frequency envelope detector (RFED) to convert the RF signal into a more detectable LF signal. As a result, most WuRxs can only receive amplitude-modulated signals [6]. On-off keying (OOK), a simplified form of amplitude modulation, is used by 85% of RF WuRxs, as determined in a large-scale literature review.

Like all modulation schemes, the bandwidth requirement for WuPts depends on the maximum frequency of the baseband signal. Symbol rates for WuPts are typically lower than those in data communication [6]. However, we found multiple articles in the literature utilizing symbol rates above 100 ksym/s, requiring a baseband frequency of at least 50 kHz [11]–[15].

In our research group, we primarily work with WuRxs based on low-frequency pattern matchers (LFPMs). LFPMs are specialized ICs, typically developed for keyless car entry systems, that can receive signals in the LF range (15–150 kHz) and perform pattern matching. Combined with a passive RFED, this enables the design of highly sensitive, reliable, and low-power WuRxs with addressing capabilities, requiring only a few additional components [7].

However, LFPM-based WuRxs require special WuPts in which the output of the RFED meets the LFPM's requirements. These requirements are illustrated in Fig. 1. Since both the RFED and LFPM act as envelope detectors, the WuPt requires double amplitude modulation. The RF carrier is turned on and off repeatedly to generate the LF carrier, while the LF envelope contains the preamble and address information of the WuPt.

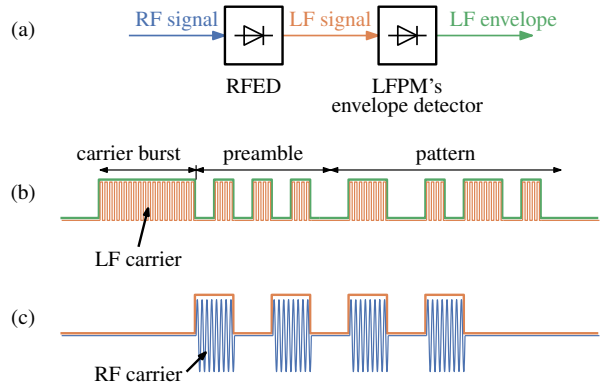

Fig. 1. Requirements on the WuPt for LFPM-based WuRxs. (a) Simplified reception path containing two envelope detectors. (b) LF envelope and LF signal of the WuPt. Visualization of the different components of the WuPt. (c) LF signal generated by the envelope of the RF signal.

In [16], we focused on minimizing the duration of the WuPt. We defined the LF modulation ratio β_{LF} as the ratio between the LF carrier f_{LF} and the symbol rate f_{sym}.

$$\beta_{\mathrm{LF}} = f_{\mathrm{LF}} / f_{\mathrm{sym}} \tag{1}$$

We also reviewed the literature for common values of β_{LF}, finding a range from 4 to 45. Fig. 1(b) and (c) illustrates $\beta_{\mathrm{LF}} = 4$, where there are four periods of the orange LF signal within each symbol represented by the green envelope.

Due to the double amplitude modulation and the LF modulation ratio, the LF of the WuPt is significantly higher than its symbol rate. Our review literature found several articles using an LF over 100 kHz. These articles are listed below, with only the first author referenced: [10], [17]–[27]. Using the LFPM AS3933, lower LF values between 11–25 kHz can be achieved [7], [28]. However, as our analysis shows, the bandwidth of the WuPt remains high due to the nature of OOK.

Few articles describe their wake-up transmitter (WuTx) design. References [29]–[31] explored using IEEE 802.11 transmitters to output a WuPt, generating an RF pulse on the WuRx channel using IEEE 802.11 frames. However, these articles did not measure the bandwidth of the generated signals.

Gavrikov et al. [28] proposed a WuRx capable of receiving frequency-shift keying (FSK) WuPts in the 2.45 GHz band. FSK-capable WuRxs based on COTS components rely on multiple RFEDs sensitive to different carrier frequencies. By switching between two carrier frequencies, a differential signal can be created. Gavrikov et al. described how to generate the WuPt using two Bluetooth Low Energy transmitters, as a single transmitter could not achieve the frequency deviation required for the WuRx. However, the bandwidth requirements of each transmitter's signal were not measured.

Del Prete et al. [32] proposed narrowing the width of an OOK pulse to concentrate more RF energy in a shorter time. The study demonstrated that improving the link budget of WuRx communication is possible, as these signals result in higher output voltages at the RFED. The authors ensured that the average power (AP) of the WuPt remained constant, while the peak envelope power (PEP) was increased. Although the authors simulated the WuPt bandwidth requirements, they did not perform measurements. With a symbol rate of 1 ksym/s and an OOK pulse width of 125 µs, the simulated bandwidth reached 140 kHz.

In this article, we will theoretically derive the spectrum of different WuPts and measure the bandwidth of WuPts generated by various RF transmitters. We will analyze the bandwidth according to European regulations. For each transmitter, we will apply different shaping filters and examine their impact on bandwidth.

III. Theory

For the following analysis and numerical calculations, we observe the baseband signal in the frequency domain. The baseband signal fully describes the behavior of the RF signal, as the only difference is a frequency shift from DC to RF by multiplying the time-domain signal by the carrier frequency. However, all measurements were taken at a carrier frequency of 868 MHz.

To achieve amplitude modulation without phase shifts, all baseband signals must remain positive. For simplicity, we set the maximum amplitude to 1. As a first step, we analyzed the amplitude modulation of a sine signal. To ensure the sine wave fits within the amplitude limits $[0,1]$, its amplitude must be raised and scaled.

$$x_1(t) = 0.5 + 0.5 \sin \omega_0 t \tag{2}$$

When analyzing the double-sided amplitude spectrum of this signal, the sine function is converted to two complex exponential functions.

$$x_1(t) = 0.5 + 0.5\left(\frac{\exp(\mathrm{j}\omega_0 t) - \exp(-\mathrm{j}\omega_0 t)}{2\mathrm{j}}\right) \tag{3}$$

This explains the peaks seen in the amplitude spectrum of the sine signal in Fig. 2. At DC, the amplitude is $-6.02\,\mathrm{dB}$, while both fundamental frequencies $\pm f_0$ have an amplitude of $-12.04\,\mathrm{dB}$.

For the square-wave signal $x_2(t)$ shown in (4), the Fourier series is given in (5).

$$x_2(t) = \begin{cases} 1, & 0 < \omega_0 t < \pi \\ 0, & \pi < \omega_0 t < 2\pi \end{cases} \tag{4}$$

$$x_2(t) = 0.5 + \sum_{n=0}^{\infty} \frac{2}{(2n+1)\pi} \sin(2n+1)\omega_0 t \tag{5}$$

This calculation explains why peaks occur only at odd multiples of the fundamental frequency. The amplitude of the harmonics decreases only slowly. The time domain and frequency domain of the square-wave signal are visualized in Fig. 2.

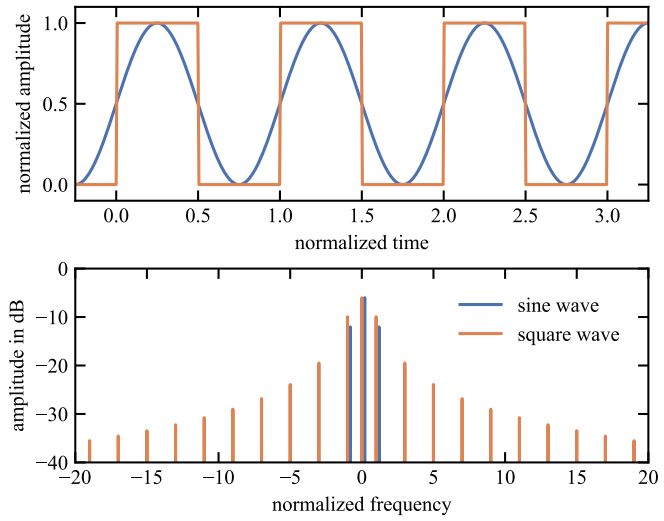

Fig. 2. Time domain and frequency domain of simple sine and square-wave signals

As presented in Section II, the LFPM WuPt uses double amplitude modulation. To analyze the spectrum of the LFPM WuPt, we opted for numerical calculations. The LF envelope of the WuPt contains the address information. However, to simplify the spectrum analysis, we used a continuous alternating pattern, like present in the preamble of the WuPt. The LF envelope here is a square-wave signal with frequency $1/2\beta_{\mathrm{LF}}$. We used $\beta_{\mathrm{LF}} = 8$ for the simulations and experiments. Since amplitude modulation is a multiplication in the time domain, the spectrum is calculated by convolution. Fig. 3 shows the time and frequency domains of the continuously modulated LFPM WuPts.

The convolution in the frequency domain is clearly visible. At each harmonic of the LF carrier, the typical amplitude modulation spectrum of the LF envelope forms. Shaping the pulses of the WuPt has a clear advantage in bandwidth reduction. For the shaped WuPt, the spectrum is largely confined to a bandwidth of $4f_0$. For the unshaped WuPt with square-wave RF pulses, the spectrum is significantly wider, with substantial spectral components at every odd multiple of f_0 due to the convolution of the two square-wave spectra.

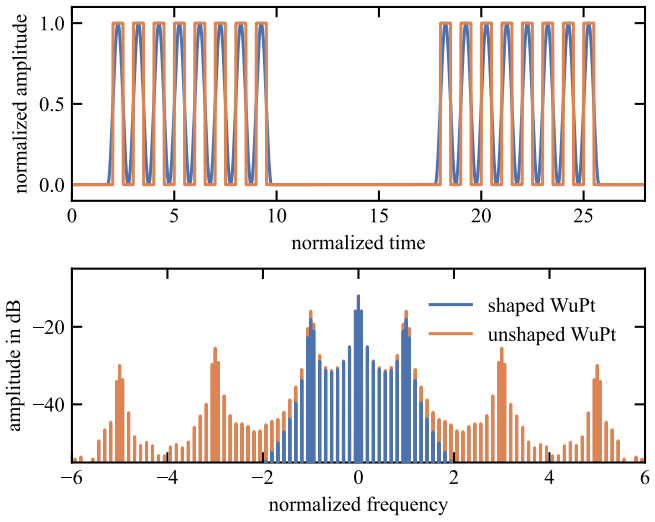

Fig. 3. Time domain and frequency domain of continuously modulated WuPts

Finally, we analyzed the spectrum of the WuPt with random data. For LFPM-based WuRxs, Manchester coding is typically used. We analyzed the double amplitude modulation with a randomly Manchester-coded signal.

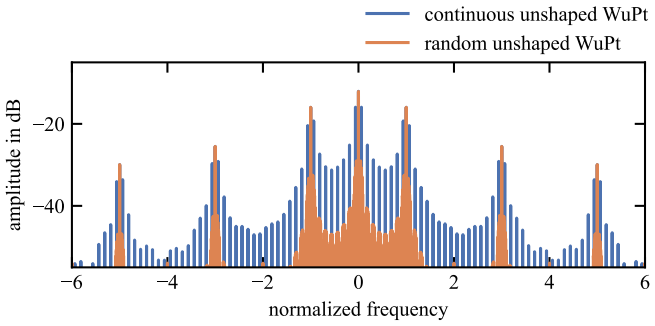

Fig. 4. Amplitude spectrum of continuous and random WuPt. The unshaped signals were used here.

Fig. 4 shows the difference between continuous and random WuPts using unshaped signals. For the random WuPt, frequency components are spread out more evenly, as is typical for random signals (e.g., white Gaussian noise). For the continuously modulated signal, the energy is concentrated in frequency bins. The continuous modulation represents the worst-case spectrum, as it produces the highest peaks. Therefore, in our experiments, we will use continuously modulated signals to ensure that all WuPts with any address information meet the bandwidth requirements.

IV. Methodology

In [7], we proposed an LFPM-based WuRx working at 868 MHz. It utilizes an LF of 18.72 kHz and LF modulation ratio β_{LF} of 8. Therefore, the symbol rate is 2.34 ksym/s. The signals analyzed here will use these parameters.

We compare the amplitude spectrum and bandwidth requirements of three different RF transmitters. The first is the Rohde & Schwarz SMCV100B vector signal generator [33]. The second is the RF transceiver IC SPIRIT1, commonly used in our sensor node prototypes [34], [35]. The third is the SPIRIT1's successor, the S2LP, released in 2016 and featuring additional signal shaping options [36].

Bandwidth has various definitions across research and industry. In this article, we focus on the regulation-oriented definition of bandwidth. We measured the WuPt bandwidth according to ETSI norms, following the guidelines in the application guide [37]. We set the WuTx to continuous transmission and used a spectrum analyzer with a resolution bandwidth of 1 kHz. Based on the ETSI limit for adjacent channel power, we used a threshold of −37 dBm to define the WuPt bandwidth. We captured the spectrum and identified the signal components above the −37 dBm level to determine the bandwidth, averaging 1000 captures to minimize measurement noise. Our measurements were conducted using a Rohde & Schwarz ZNL6 spectrum analyzer [38].

For amplitude-modulated signals, the carrier is fully or partially turned off for a set period. Consequently, the peak envelope power (PEP) is greater than the average power (AP) of the signal, and the ratio between these values is known as the peak-to-average power ratio (PAPR).

The maximum allowable transmit power for the 868 MHz band is 14 dBm. Measurements with the SMCV100B were conducted with a PEP of 14 dBm, confirmed using the IQ analyzer to view the time-domain baseband signal. The RF power level programmed into the SMCV100B are typically AP values. However, this is not true for all configuration. For example, for analog amplitude modulation, it represents the carrier power.

For RF transceiver ICs, the maximum transmit power is limited by the IC, matching circuit, and PCB traces. We measured a PEP of 7.9 dBm for the SPIRIT1 and 12.9 dBm for the S2LP. These PEP differences impact the measured bandwidth and should be considered.

V. Results

Fig. 5 shows the measured spectra of unshaped WuPts, with the −37 dBm threshold for bandwidth marked as a horizontal line. The bandwidths for each signal are shown as lines at the bottom of the plot.

The measured bandwidths were 340 kHz for the SMCV100B, 937 kHz for the SPIRIT1, and 524 kHz for the S2LP. The SMCV100B had the lowest bandwidth, while the SPIRIT1's bandwidth was approximately triple due to sharper transitions in the OOK modulator. The bandwidth requirements are 18 to 50 times larger than the baseband frequency.

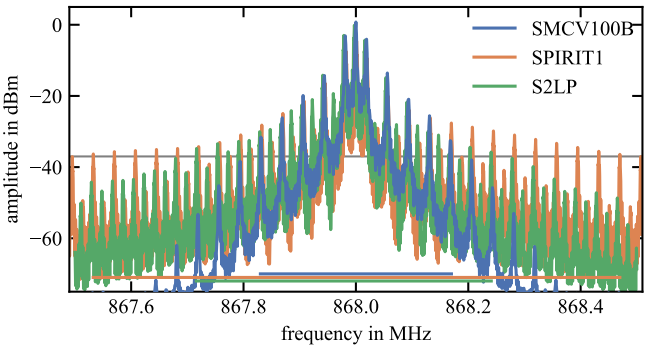

Fig. 5. Measured amplitude spectrum of continuous WuPts without shaping

We repeated the measurement using an LF of 125 kHz, another common LF in LFPMs as discussed in Section II. The measured bandwidths were 2.27 MHz for the SMCV100B and 4.76 MHz for the SPIRIT1. The S2LP does not support an OOK data rate of 250 kbit/s, which is needed for generating the 125 kHz signal.

The shaping filter theoretically analyzed in Section III is a raised-cosine filter, using cosine waves to shape the WuPt pulses. We configured the raised-cosine filter option on the SMCV100B. Fig. 6 shows the spectra of the SMCV100B signals, with and without shaping.

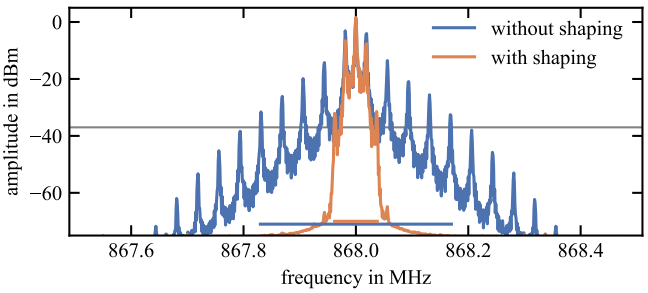

Fig. 6. Measured amplitude spectrum of continuous WuPts generated by SMCV100B vector signal generator

The SMCV100B's shaping filter significantly reduced the bandwidth, decreasing it from 340 kHz to 76 kHz. The SMCV100B achieves a near-ideal spectrum, where the bandwidth is only four times the LF, as predicted in Section III.

The SPIRIT1's power amplifier can be configured to shape the OOK signal output, with eight output levels available. Two levels are reserved for minimum and maximum power. We used raised-cosine coefficients for the remaining six, calculating attenuation values of $[26.0, 14.5, 8.0, 4.0, 1.8, 0.5]$ dB. Fig. 7 compares the spectra of the SPIRIT1 signals, with and without shaping.

The SPIRIT1 was able to reduce the bandwidth from 937 kHz to 610 kHz. Fig. 8 visualizes the shaped time-domain baseband signal. This figure shows sharp transitions when switching between power levels. These edges are responsible for the high bandwidth of te shaped WuPt.

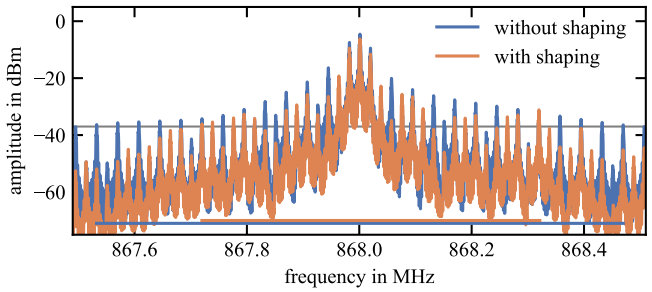

Fig. 7. Measured amplitude spectrum of continuous WuPts generated by SPIRIT1 transceiver IC

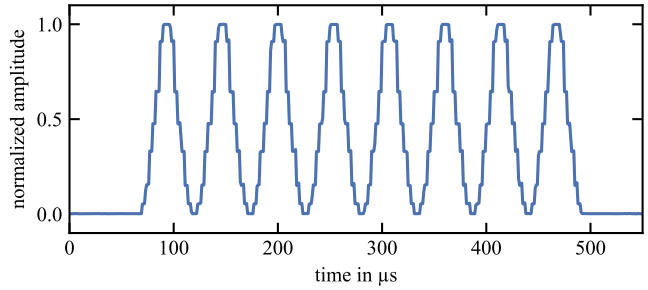

Fig. 8. Shaped time-domain baseband signal of SPIRIT1. The transitions between the different output levels of the power amplifier are clearly visible.

The S2LP's power amplifier offers similar ramping options as the SPIRIT1 but additionally includes a digital filter specifically designed to shape the OOK modulated signal. The filter's cutoff frequency can be set to $[12.5, 25, 50, 100]$ kHz. We found that the 12.5 and 25 kHz options attenuated the output signal. Fig. 9 shows the spectrum of the 25 kHz filter compared to the unshaped signal.

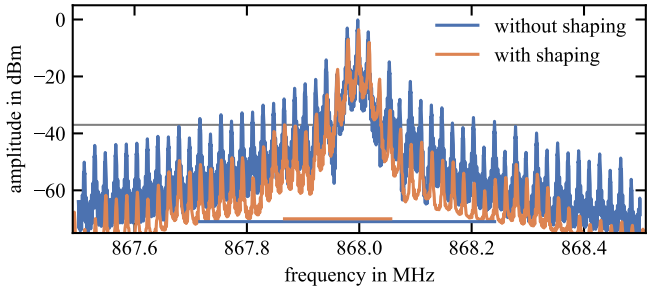

Fig. 9. Measured amplitude spectrum of continuous WuPts generated by S2LP transceiver IC

The S2LP's output filter reduced the bandwidth from 524 kHz to 189 kHz. Comparing Fig. 6 and 9, the S2LP is not as effective as the lab-grade SMCV100B in bandwidth reduction, but it achieves a reduction to $10 f_0$.

VI. Conclusion and Discussion

This article focuses on wake-up receivers (WuRxs) based on commercial off-the-shelf components. Most of these WuRxs can only receive OOK signals because they use passive radio-frequency envelope detectors. A subcategory of these WuRxs employs low-frequency pattern matchers (LFPMs), which are ICs capable of receiving LF signals in the 15–150 kHz range. Due to the RFED and the LFPM, there are two envelope detectors in the reception path, requiring double amplitude modulation of the wake-up packet (WuPt), as shown in Fig. 1.

In Section II, we analyzed the current research and highlighted that LFPMs are widely used. Multiple references use LF values over 100 kHz, resulting in high bandwidth for the WuPt. We found that few articles focus on the generation of the WuPts. Only Del Prete et al. [32] provided a simulation of WuPt bandwidth.

In Section III, we performed calculations and numerical analysis to illustrate the spectrum of different signals. In particular, we showed that a square-wave signal has a high bandwidth.

In Section V, we presented the results of our bandwidth measurements. With an LF of 18.7 kHz, the bandwidth of an LFPM WuPt ranged from 340–937 kHz, depending on the transceiver used. Due to the sharp transitions of OOK modulation, the bandwidth is up to 50 times larger than the LF. With an LF of 100 kHz (as per Section II), a bandwidth in the range of 5 MHz is reached.

By enabling signal shaping on three different RF transmitters, we were able to significantly reduce the bandwidth. For the lab-grade vector signal generator SMCV100B, the bandwidth decreased from 340 kHz to 76 kHz. For the SPIRIT1 RF transceiver IC, the bandwidth decreased from 937 kHz to 601 kHz [35]. The SPIRIT1's successor, the S2LP, supports additional shaping options and achieved a substantial reduction in bandwidth, decreasing from 524 kHz to 189 kHz. However, the S2LP still did not match the bandwidth reduction achieved by the SMCV100B.

Generally, wireless sensor nodes should operate in license-free frequency bands, as unlicensed bands are essential for broad applications of sensor networks. Bandwidth requirements are important to ensure that the WuPt fits into the utilized RF band. The 2.45 GHz band spans over 100 MHz and allows for wideband WuPts. The 868 MHz band spans a total of 7 MHz, but is divided into multiple sub-bands with different requirements. Spanning a WuPt across multiple sub-bands is not recommended, as overlapping regulations severely limit the allowable duty cycle and transmission power. The 434 MHz band spans 1.74 MHz in total. [39] This frequency band is used in studies such as [10], [20], [25]. WuPts with LF of 100 kHz cannot legally transmitted in this band, as their bandwidth can reach 5 MHz. Additional filtering would be needed to reduce out-of-band emissions. For 125 kHz WuPts, we measured bandwidths of 2.27 MHz for the SMCV100B and 4.76 MHz for the SPIRIT1. These WuPts do not fit in the 434 MHz band.

Pulse shaping generally increases the peak-to-average power ratio (PAPR) by reducing the transmitter's output power during ramping. Future research should investigate the impact of increased PAPR on WuRx sensitivity.

References

[1] J. Braun and F. Derbel, "Wireless sensor network for fire detection with network coding to improve security and reliability," 2024.

[2] O. Kanoun, S. Bradai, S. Khriji, G. Bouattour, D. El Houssaini, M. Ben Ammar, S. Naifar, A. Bouhamed, F. Derbel, and C. Viehweger, "Energy-aware system design for autonomous wireless sensor nodes: A comprehensive review," *Sensors*, vol. 21, no. 2, 2021.

[3] R. Fromm, L. Schott, and F. Derbel, "Improved wake-up receiver architectures with carrier sense capabilities for low-power wireless communication," in *Sensor Networks*, A. Ahrens, R. V. Prasad, C. Benavente-Peces, and N. Ansari, Eds. Cham: Springer International Publishing, 2022, pp. 60–84.

[4] M.-C. Ziesmann, C. Fühner, and F. Büsching, "Hotwire– decreasing latency between wake-up calls in semi-active WUR-scenarios," in *2023 IEEE 12th International Conference on Intelligent Data Acquisition and Advanced Computing Systems: Technology and Applications (IDAACS)*, vol. 1, 2023, pp. 655–660.

[5] G. Liu, T. Ma, W. Yin, J. Zhang, H. Gao, and B. Wu, "A 2.4GHz band highly sensitive low power wake-up receiver," in *2023 International Conference on Ubiquitous Communication (Ucom)*, 2023, pp. 116–120.

[6] R. Piyare, A. L. Murphy, C. Kiraly, P. Tosato, and D. Brunelli, "Ultra low power wake-up radios: A hardware and networking survey," *IEEE Communications Surveys Tutorials*, vol. 19, no. 4, pp. 2117–2157, 2017.

[7] R. Fromm, O. Kanoun, and F. Derbel, "An improved wake-up receiver based on the optimization of low-frequency pattern matchers," *Sensors*, vol. 23, no. 19, 2023.

[8] S. Hmidi, R. Fromm, R. Barrak, and F. Derbel, "Experimental investigations on RF filters in wake-up receiver circuits," in *2024 21st International Multi-Conference on Systems, Signals & Devices (SSD)*, 2024, pp. 286–291.

[9] A. Sánchez, S. Blanc, P. Yuste, A. Perles, and J. J. Serrano, "An ultra-low power and flexible acoustic modem design to develop energy-efficient underwater sensor networks," *Sensors*, vol. 12, no. 6, pp. 6837–6856, 2012.

[10] G. U. Gamm, S. Stoecklin, and L. M. Reindl, "Wake-up receiver operating at 433 MHz," in *2014 IEEE 11th International Multi-Conference on Systems, Signals Devices (SSD14)*, 2014, pp. 1–4.

[11] C. Petrioli, D. Spenza, P. Tommasino, and A. Trifiletti, "A novel wake-up receiver with addressing capability for wireless sensor nodes," in *2014 IEEE International Conference on Distributed Computing in Sensor Systems*, 2014, pp. 18–25.

[12] E. Lopez-Aguilera, M. Hussein, M. Cervia, J. Paradells, and A. Calveras, "Design and implementation of a wake-up radio receiver for fast 250 kb/s bit rate," *IEEE Wireless Communications Letters*, vol. 8, no. 6, pp. 1537–1540, 2019.

[13] Y. Ammar, S. Bdiri, and F. Derbel, "An ultra-low power wake up receiver with flip flops based address decoder," in *2015 IEEE 12th International Multi-Conference on Systems, Signals Devices (SSD15)*, 2015, pp. 1–5.

[14] S. Bdiri, F. Derbel, and O. Kanoun, "A tuned-RF duty-cycled wake-up receiver with -90 dBm sensitivity," *Sensors*, vol. 18, no. 1, 2018.

[15] B. Yi, F. Wang, C. Huang, X. Cao, and K. Li, "A low-cost and low-power 2.4 GHz wake-up receiver," in *2022 IEEE 10th Asia-Pacific Conference on Antennas and Propagation (APCAP)*, 2022, pp. 1–2.

[16] R. Fromm, O. Kanoun, and F. Derbel, "Quasi-real-time wireless communication based on wake-up receivers with a latency below 5 ms," in *2024 IEEE International Instrumentation and Measurement Technology Conference (I2MTC)*, 2024, pp. 1–6.

[17] E. Umbdenstock, F. Schaefer, M. Kleinsteuber, and H. Meyer, "Wake-up-receiver in energy efficient wireless sensor networks for security applications," 2012.

[18] T. V. Prabhakar, N. S. Soumya, P. Muralidharan, and H. S. Jamadagni, "A novel wake-up radio WSN mote," in *2013 Texas Instruments India Educators' Conference*, 2013, pp. 362–368.

[19] T. Kumberg, C. Schindelhauer, and L. Reindl, "Exploiting concurrent wake-up transmissions using beat frequencies," *Sensors*, vol. 17, no. 8, 2017.

[20] S. Babatunde, A. Alsubhi, J. Hester, and J. Sorber, "Greentooth: Robust and energy efficient wireless networking for batteryless devices," *ACM Trans. Sen. Netw.*, vol. 20, no. 3, apr 2024.

[21] M. Hierold, R. Weigel, and A. Koelpin, "Assessment of transmitter initiated wake-up radio versus pure wake-up receiver decoding," *IEEE Microwave and Wireless Components Letters*, vol. 27, no. 4, pp. 413–415, 2017.

[22] A. Bannoura, "Algorithms and applications for low power wireless sensor networks using wake-up receivers," 2016.

[23] J. Blobel, J. Krasemann, and F. Dressler, "An architecture for sender-based addressing for selective sensor network wake-up receivers," in *2016 IEEE 17th International Symposium on A World of Wireless, Mobile and Multimedia Networks (WoWMoM)*, 2016, pp. 1–7.

[24] F. Pflaum, R. Weigel, and A. Koelpin, "Ultra-low-power sensor node with wake-up-functionality for smart-sensor-applications," in *2018 IEEE Topical Conference on Wireless Sensors and Sensor Networks (WiSNet)*, 2018, pp. 107–110.

[25] F. Sutton, "Ultra-low power wireless hierarchical sensing," Master's thesis, ETH Zurich, 2012.

[26] D. Galante-Sempere, D. Ramos-Valido, S. Lalchand Khemchandani, and J. del Pino, "Low-power RFED wake-up receiver design for low-cost wireless sensor network applications," *Sensors*, vol. 20, no. 22, 2020.

[27] C. Mc Caffrey, T. Sillanpää, H. Huovila, J. Nikunen, S. Hakulinen, and P. Pursula, "Energy autonomous wireless valve leakage monitoring system with acoustic emission sensor," *IEEE Transactions on Circuits and Systems I: Regular Papers*, vol. 64, no. 11, pp. 2884–2893, 2017.

[28] P. Gavrikov, P. E. Verboket, T. Ungan, M. Müller, M. Lai, C. Schindelhauer, L. M. Reindl, and T. Wendt, "Using bluetooth low energy to trigger an ultra-low power FSK wake-up receiver," in *2018 25th IEEE International Conference on Electronics, Circuits and Systems (ICECS)*, 2018, pp. 781–784.

[29] Y. Kondo, H. Yomo, S. Tang, M. Iwai, T. Tanaka, H. Tsutsui, and S. Obana, "Energy-efficient WLAN with on-demand AP wake-up using IEEE 802.11 frame length modulation," *Computer Communications*, vol. 35, no. 14, pp. 1725–1735, 2012, special issue: Wireless Green Communications and Networking.

[30] J. Oller, E. Garcia, E. Lopez, I. Demirkol, J. Casademont, J. Paradells, U. Gamm, and L. Reindl, "IEEE 802.11-enabled wake-up radio system: design and performance evaluation," *Electronics Letters*, vol. 50, no. 20, pp. 1484–1486, 2014.

[31] E. Lopez-Aguilera, I. Demirkol, E. Garcia-Villegas, and J. Paradells, "IEEE 802.11-enabled wake-up radio: Use cases and applications," *Sensors*, vol. 20, no. 1, 2020.

[32] M. Del Prete, A. Costanzo, M. Magno, D. Masotti, and L. Benini, "Optimum excitations for a dual-band microwatt wake-up radio," *IEEE Transactions on Microwave Theory and Techniques*, vol. 64, no. 12, pp. 4731–4739, 2016.

[33] "R&S SMCV100B vector signal generator," Rhode&Schwarz, Oct. 2024, specifications version 16.00.

[34] M. Weber, G. Fersi, R. Fromm, and F. Derbel, "Wake-up receiver-based routing for clustered multihop wireless sensor networks," *Sensors*, vol. 22, no. 9, 2022.

[35] "SPIRIT1 - Low data rate, low power sub-1GHz transceiver," STMicroelectronics NV, Oct. 2016.

[36] "S2-LP: Ultra-low power, high performance, sub-1 GHz transceiver," STMicroelectronics, 2023, datasheet, revision 11.

[37] P. D. Vita, "Using the SPIRIT1 transceiver under EN 300 220 at 868 MHz," STMicroelectronics, Jul. 2012, application note AN4110.

[38] "R&S ZNL vector network analyzer," Rhode&Schwarz, Sep. 2024, specifications version 9.00.

[39] "Frequenzplan," Bundesnetzagentur, Mar. 2022.